International Journal of GEOMATE, April, 2025 Vol.28, Issue 128, pp.108-116
ISSN: 2186-2982 (P), 2186-2990 (O), Japan, DOI: https://doi.org/10.21660/2025.128.4925
Geotechnique, Construction Materials and Environment

CYCLIC LOAD-DRIFT BEHAVIOR OF EXTERIOR BEAM-COLUMN JOINTS RETROFITTED WITH ULTRA-HIGH-PERFORMANCE CONCRETE

*Trung-Hieu Tran

[1]Faculty of Civil Engineering, Hanoi Architectural University, Hanoi 100000, Vietnam

*Corresponding Author, Received: 19 Feb. 2025, Revised: 28 March 2025, Accepted: 31 March 2025

ABSTRACT: Exterior beam-column joints play a crucial role in the seismic performance of reinforced concrete (RC) frame structures, yet the application of Ultra High Performance Concrete (UHPC) for strengthening them remains limited despite its potential. This study evaluates UHPC's effectiveness in enhancing the load capacity and seismic behavior of these joints. Three full-scale specimens—one conventional RC joint designed for high ductility (DCH) per Eurocode 8, and two UHPC-retrofitted joints without stirrups—were tested under cyclic loading. The UHPC-retrofitted joints exhibited load capacities 18.9% and 24.5% greater than the control, along with improved drift and energy dissipation. These findings demonstrate UHPC's potential to enhance seismic resilience and offer a viable retrofitting solution for RC structures in earthquake-prone regions. However, the limited use of UHPC highlights the need for further research to promote its broader adoption in structural design.

Keywords: UHPC; Exterior joint; Reversed cyclic loading; Seismic loading; Dynamic responses

1. INTRODUCTION

Reinforced concrete (RC) frame structures are widely used due to their construction speed, cost efficiency, and flexibility [1], with beam-column joints playing a critical role in maintaining stability under seismic forces [2]. However, exterior joints face challenges from shear cracking, anchorage slippage, and joint core crushing under cyclic loading [3, 4], exacerbated by their lower shear capacity compared to interior joints [5]. Insufficient anchorage length and lack of transverse stirrups often lead to joint failure in earthquake-prone regions [6], prompting strict design standards like Eurocode 8 for high ductility (DCH) joints [7]. Yet, dense reinforcement can complicate construction [8].

To address these issues, advanced materials such as polymer-based systems like Fiber Reinforced Polymers (FRP) (offering high tensile strength and corrosion resistance) and cement-based Ultra High Performance Concrete (UHPC) (with exceptional compressive strength, durability, and fiber-enhanced ductility) have been utilized to improve the shear resistance of exterior joints, surpassing conventional concrete's limitations [9, 10]. Several publications have discussed experimental investigations aimed at enhancing the seismic resistance capacity of exterior joints using these innovative materials, with all authors agreeing that such strengthening techniques can positively impact the earthquake resilience of frame joints [11-14]. Nevertheless, these techniques have drawback, including increased joint size due to retrofitting layers, challenges in implementing connections in confined spaces, corrosion of reinforced plates, degradation of the epoxy layer leading to detachment of retrofitting plates, and poor heat resistance of polymeric materials [15-16]. Röhm et al. [17] conducted tests on three groups of external joints subjected to seismic effects. Group 1 comprised specimens designed according to Indian standards [18] and Eurocode 8 [7] with a medium ductility class (DCM). Group 2 included specimens retrofitted with steel fibers at a ratio of 1% to 1.5%, combined with higher-strength concrete, to assess the influence of fiber content and concrete strength on the seismic performance of joints [19]. Group 3 was reinforced with HPFRC to shift plastic hinges from the column to the beam [20]. Results indicated that HPFRC external joints demonstrate greater durability and energy dissipation during seismic activity compared to conventional concrete joints, representing an early effort to explore UHPC and HPFRC applications in seismic retrofitting [21]. Furthermore, while UHPC's superior mechanical properties, such as compressive strengths exceeding 120 MPa and enhanced toughness, are well-documented [22], its advantages over other strengthening methods, like FRP or steel jacketing, for exterior beam-column joints remain underexplored, particularly in terms of seismic energy dissipation and construction simplicity [23-24].

Additionally, the incorporation of fibers into the UHPC matrix enhances ductility, a critical characteristic for structural members subjected to earthquake loads [25]. The use of UHPC to increase the load capacity of structural members exemplifies its potential application in the structural retrofit sector [26, 27]. Recent research by Sharma et al. and Khan et al. has investigated the performance of UHPC-retrofitted exterior joints under cyclic loading [28, 29], indicating improved ductility and energy dissipation during seismic activity. However, these

studies focused solely on using UHPC as retrofitting layers within the joint core zone, leaving gaps in understanding its broader seismic enhancement potential [30]. Other studies have explored UHPC's tensile strength under high strain rates [31] and its behavior under elevated temperatures [32], further supporting its versatility.

Despite UHPC's promise, prior research has often concentrated on interior joints or broader structural elements rather than specific seismic enhancements for exterior joints [33, 34]. The main purpose of this study is to experimentally and analytically evaluate UHPC's effectiveness in improving the cyclic load-drift behavior and load capacity of exterior beam-column joints, addressing these knowledge gaps to inform seismic design practices [35, 36].

The remaining sections of the paper is constructed as following. Section 2 outlines the study's contributions to seismic resilience and construction practices. Section 3 details the experimental design, including specimen preparation, material properties, and cyclic loading protocols, providing the foundation for the investigation. Section 4 presents the findings, comparing load capacities, ductility, and energy dissipation across the control and UHPC-retrofitted specimens, supported by load-displacement curves and failure mode analyses. Finally, the "Conclusions" section synthesizes the results, discusses practical implications, and offers insights into the feasibility of large-scale UHPC adoption, highlighting areas for future research.

2. RESEARCH SIGNIFICANCE

This study evaluates the cyclic load-drift behavior of exterior beam-column joints retrofitted with Ultra High Performance Concrete (UHPC), providing a comprehensive analysis of load-displacement relationships, failure modes, energy dissipation capacity, and overall seismic performance. The findings offer valuable insights into how UHPC can enhance the resilience of reinforced concrete (RC) structures under earthquake loads. This retrofitting approach could simplify construction by reducing reinforcement congestion, making it more efficient and cost-effective. Additionally, UHPC's long-term durability may extend the lifespan of structures, while its environmental impact could be minimized through optimized material use. Although the production of UHPC requires higher energy, its cost-effectiveness may balance initial expenses with reduced maintenance and repair needs over time.

3. TESTING PROGRAM

3.1 Test Specimens and Material

In the present study, the 1:1 scale test specimens are designed in accordance with Eurocode 8 [39] and represent an exterior joint of a three-story building with a total height of 9.9 meters. The rectangular plan measures 30 meters by 24 meters, as illustrated in Fig.1. All specimens share equivalent geometric characteristics. The beams are 2000 mm long with a cross-sectional area of 350 mm by 450 mm. while the columns are 3300 mm high with a cross-sectional dimension of 350 mm by 350 mm. Specimen S1 serves as the control specimen without UHPC retrofitting and utilizes steel stirrups with a diameter of 10 mm and a spacing of 100 mm. In contrast, specimens S2 and S3 are retrofitted with UHPC at the joints instead of using transverse reinforcements. The UHPC retrofit extends 450 mm in specimen S2, while in specimen S3, it measures 675 mm. Fig. 2 provides detailed illustrations of the test specimens. However, this study only utilized three specimens, which may not fully capture the diverse configurations or combined conditions—such as varying beam-column ratios or environmental exposures—encountered in real-world applications. Additionally, assessing the durability and longevity of UHPC-retrofitted joints under prolonged seismic or environmental stress remains critical but unaddressed here.

Fig.1 Design of three-storey building including exterior joints

This investigation employs steel reinforcement of type CB400-V, which meets the requirements for structures classified with a high ductility grade (DCH). The mechanical characteristics of the steel reinforcing bars are presented in Table 1. The compressive strength of the conventional concrete specimens is measured at 58.4 MPa. As detailed in Table 2, UHPC is produced in Vietnam using locally available materials, including cement, silica fume, fine sand, and 2% steel fibers. The mechanical properties of UHPC, including compressive strength, direct tensile strength, and modulus of elasticity. are assessed through testing procedures that adhere to ASTM and AFGC-SETRA [19] specifications. The mechanical properties of the UHPC are summarized in Table 3. UHPC's direct tensile strength of 8.1 MPa (Table 3) aided crack control in retrofitted joints. Fracture toughness tests were omitted due to time limitations and emphasis on cyclic loading response.

Future work will incorporate these tests to investigate post-cracking behavior and further validate UHPC's effectiveness. UHPC's compressive strength of 122.93 MPa (Table 3), exceeding twice that of conventional concrete (58.4 MPa), enhanced joint capacity. Microstructural analysis via SEM was excluded due to lack of equipment and the study's emphasis on macroscopic seismic behavior. Future research will employ SEM to validate strength enhancements at the microstructural level. Additionally, the 2% steel fibers in UHPC (Table 2) delayed crack propagation, enhancing ductility in retrofitted joints. Fiber orientation analysis via X-ray computed tomography was not conducted due to limited resources and emphasis on load-drift behavior. Future studies will use CT to explore microstructural fiber effects and improve understanding of UHPC's performance.

Table 1 Mechanical properties of steel reinforcing bars

Nominal bar Diameter (mm)	Yield strength (MPa)	Ultimate strength (MPa)	Elastic modulus (GPa)
10	585	701	
20	577	695	200
25	528	662	

Table 2 UHPC mix composition

Cement	Water	Silica fume	Fine sand	Superplasticize (%)	Fiber (%)
886	162	222	1109	39.5	2.0

Table 3 Mechanical properties UHPC material

Parameter	Unit	Value
Compressive strength	MPa	122.93
Direct tensile strength	MPa	8.1
Modulus of elasticity	MPa	41946
Poisson's ratio	//	0.2

3.2 Fabrication of the Testing Specimens

During the fabrication process, a thin wooden plate is used as a barrier in specimens S2 and S3 to separate the conventional concrete from the UHPC, ensuring a clear distinction between the two materials. Once the concrete has been poured and set, the plate is removed from the separation surface, and the concrete is vigorously vibrated to achieve proper compaction. After 48 hours, the formwork is removed from the concrete surface, and the specimens are allowed to cure at room temperature, as shown in Fig.3.

The dynamic jack system is responsible for inducing displacement at the end of the beam, which generates rotation angles in the structural elements and shear strain in the joint. Each test specimen is equipped with 21 symmetrically arranged displacement transducers (LVDTs) for data collection. To measure the beam-column rotation angle, four LVDTs are symmetrically installed on both sides of the beams, as illustrated in Fig. 4a. The beam-column rotation angle is calculated by dividing the difference in data between the two LVDTs by the 500 mm horizontal distance between them. The same method is used to calculate the column's rotation angle, shown in Fig. 4b. The deformation of the joint γ is detected using two diagonally positioned LVDTs, as represented in Fig. 4c. The equation for calculating is as follows:

$$\gamma = \frac{(2D + \delta_1 + \delta_2)(\delta_1 - \delta_2)}{4h_c.h_b} \quad (1)$$

where D represents the diagonal length; δ_i signifies the variable length of the LVDT; h_c and h_b denote the distances between the LVDTs; X reflects the horizontal displacement of the joint. However, relying solely on LVDTs may not fully assess subtle joint behaviors, such as microcracking or minor deformations, which could influence long-term performance.

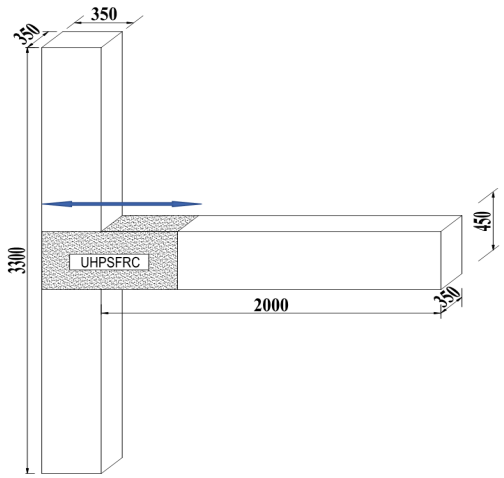

Fig.2 Detail of test specimens

Fig.3 Specimens after removing the formwork

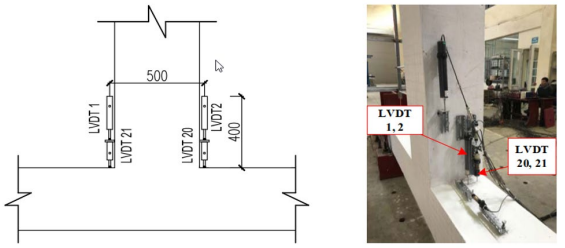

a) To measure beam-column rotation angle

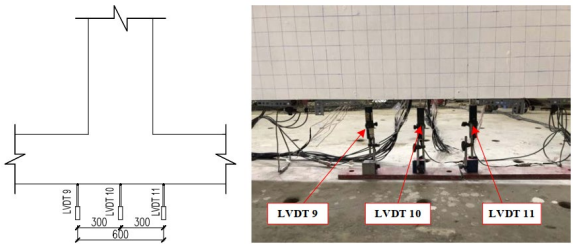

b) To measure rotation angle of column

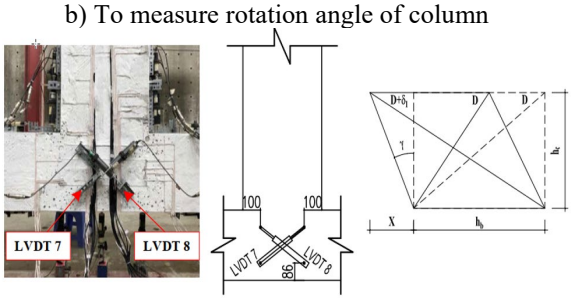

c) To measure deformation of joint

Fig.4 Layout of LVDTs in specimens

3.3 Test Setup

The test configuration for the exterior joint subjected to cyclic loading is shown in Fig. 5. In this experiment, the columns are oriented horizontally while the beams are positioned vertically, reflecting a 90-degree rotation from their original alignment. This arrangement facilitates the application of vertical loads to the column. A dynamic actuator with a capacity of 500 kN and a horizontal travel range of ±500 mm is affixed to the end of the beam, parallel to the rigid floor. Throughout the experimental procedure, a vertically mounted static loading actuator with a capacity of 1500 kN applies a constant vertical force of 650 kN to the column. Load cells are installed to monitor the vertical forces and the reaction force at the column. During the loading process, a data acquisition system is connected to a computer to record data from all linear variable differential transformers (LVDTs) and strain gauges. High-strength steel structures are used as reaction frames, securely fastened to the rigid floor with large diameter bolts. The testing setup allows only rotational displacement at both ends of the column, which is controlled by supports and rollers at either end. Additionally, each column base is bolted to the floor to prevent any out-of-plane movement.

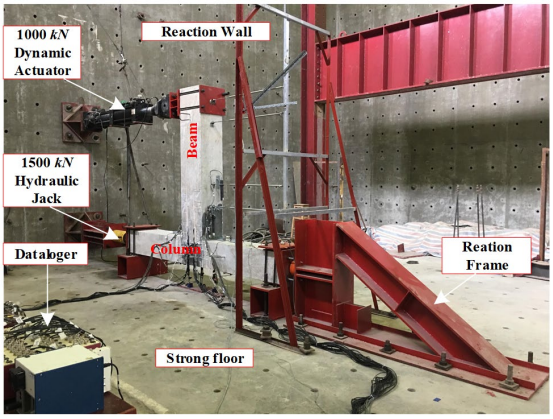

Fig.5 Test setup of specimens

3.4 Loading History

The experiment involves applying cyclic loading combined with a vertical load of 650 kN on the column head using a static loading actuator, resulting in a compression force ratio of 0.1. The loading process consists of two phases. The initial phase utilizes force control to identify the load that causes the first cracking, while the subsequent phase employs the yielding response of the steel reinforcing bars for displacement control. The loading procedure in the second phase follows the guidelines set by ACI Committee 374 [37]. This approach has been widely used in various research studies [38-40]. During this phase, the loading is applied at a frequency of 0.01 Hz to simulate static loading. Each loading step at the end of the beam consists of three cycles with identical displacements. Within the initial loading step, the displacement amplitude is adjusted to the yield displacement (Δy), which can be calculated via numerical analysis and experimental measurements. The displacement amplitudes for each subsequent loading step are afterwards defined in the following manner: 1Δy, 1.4Δy, 1.7Δy, 2.2Δy, 2.75Δy, 3.5Δy, 4Δy, 5Δy, and 6.5Δy. After the completion of the twelfth cycle, a control cycle is introduced with an amplitude equal to one-third of the previous amplitude, as shown in Fig. 6. This technique helps to mitigate potential losses attributed to stiffness degradation during the loading procedure. The amplitude increments were selected to simulate progressive seismic deformation based on typical earthquake response patterns, while the control cycle ensures data reliability under repeated loading, reflecting realistic seismic demands as per ACI Committee 374 guidelines. The drift, defined as the ratio of displacement to the length of beam, can be calculated using the following formula:

$$Drift = \frac{\Delta l}{0.5 l_b}.100\% \quad (2)$$

where Δl defines the displacement at the end of the beam; l_b denotes the length of the beam. Notably, this study tested only one cyclic load scenario with

varying UHPC lengths, limiting insights into other parameters like load intensity or frequency. Field challenges, such as UHPC adhesion to existing concrete in wet or dirty conditions, weather effects on UHPC hardening, and industry readiness to adopt this technology, were not evaluated.

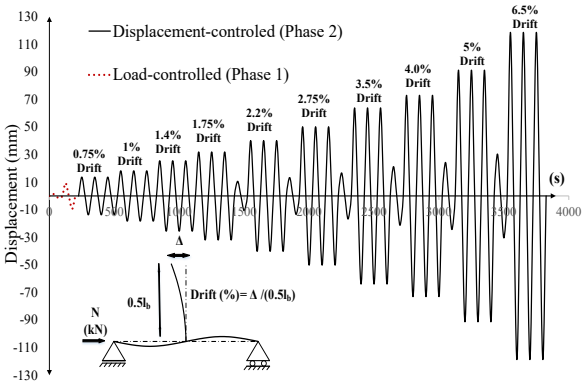

Fig.6 Loading history of cyclic test

4. EXPERIMENTAL RESULTS

The experimental results presented in Table 4, coupled with the load-displacement curves depicted in Figures 7, 8, and 9, provide valuable insights into the influence of UHPC retrofitting on the cyclic behavior of exterior beam-column joints. A comparative analysis of the three specimens—the control specimen (S1) and two UHPC-retrofitted specimens (S2 and S3 with varying retrofit lengths)—reveals significant differences in load-carrying capacity, stiffness degradation, ductility, and energy dissipation characteristics.

The control specimen (S1), constructed without UHPC reinforcement, serves as a benchmark against which to evaluate the effectiveness of the UHPC retrofitting strategies. As shown in Figure 7 and Table 4, specimen S1 exhibited a relatively linear elastic response up to a drift of approximately 1%. Beyond this point, the load-displacement curve deviates from linearity, indicating the onset of micro-cracking and stiffness degradation within the joint region. The initiation of visible cracking occurs at a drift of approximately 1.4%, as evidenced by the data in Table 4. The load capacity continues to increase until reaching a peak load of 185.8 kN at a drift of 2.2%. Beyond this point, the curve shows a steep decrease in load-carrying capacity, accompanied by significant damage, suggesting brittle failure behavior. The rapid decline in load capacity from the peak load (2.2% drift) to the end of testing (5% drift) is a clear indicator of the limited energy dissipation capacity of the conventional reinforced concrete joint. The relatively low load capacity at higher drift values emphasizes the vulnerability of unreinforced joints to significant damage under seismic loading. The observed failure mode of specimen S1 likely involved crushing of the concrete in the joint core, combined with yielding of the steel reinforcement in the anchorage zone, and potential shear failure.

The initial cracking load increased from 60 kN in S1 to 80 kN in S2 and S3 (Table 4), highlighting UHPC's ability to delay crack onset. Crack propagation was not assessed using Digital Image Correlation (DIC) due to equipment constraints and the study's focus on load-displacement behavior. Future work will employ DIC to provide detailed crack pattern analysis.

Table 4 Test results of specimens

Drift (%)	S1	S2	S3
	Loading (kN)	Loading (kN)	Loading (kN)
First crack	60	80	80
0.75	111.2	115.8	132.2
1	135.7	143.2	158.7
1.4	167.5	180.6	193.9
1.75	182.7	203.8	222.2
2.2	185.8	220.8	231.4
2.75	185.8	216.4	217.8
3.5	184.7	208	211.6
4	176.5	185.1	195.7
5	170.8	181.8	189.7
6.5		171.4	176.9

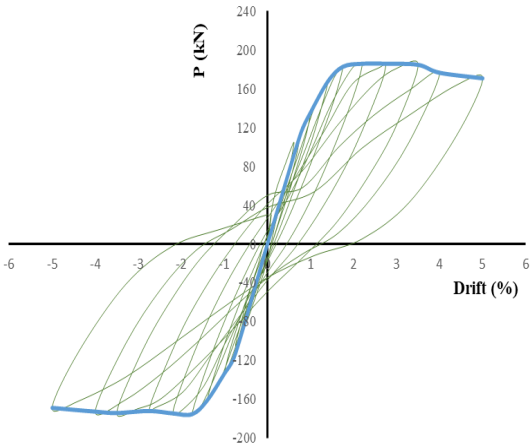

Fig.7 Load versus deformation curve of control specimen S1

Specimen S2, reinforced with a 450 mm UHPC layer, demonstrates a significant improvement in seismic performance compared to the control specimen. As illustrated in Figure 8 and Table 4, the initial elastic behavior of S2 is comparable to S1, with slight stiffness degradation observed up to 1% drift. This similarity suggests that the UHPC retrofit does not adversely affect the initial stiffness of the joint. However, in contrast to S1, the load-displacement curve for S2 exhibits a more gradual and less abrupt decline in stiffness following the onset of cracking at a drift of 1.4%. This sustained stiffness at higher drift values indicates enhanced ductility, a critical factor in improving seismic resistance. The maximum load

capacity of S2 (220.08 kN at 2.2% drift) is considerably higher than S1, representing a notable increase of 18.9%. The ability of the UHPC to effectively confine the concrete and enhance its post-cracking strength contributes significantly to this enhanced load capacity. The improved ductility, as indicated by the more gradual post-peak decline, suggests a higher energy dissipation capacity compared to the brittle failure exhibited by S1. The failure of S2 is likely delayed to higher drifts, potentially indicating a more ductile failure mode involving extensive cracking of both the concrete and the UHPC layer before complete failure.

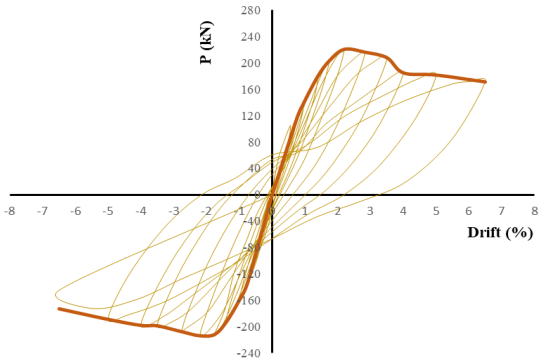

Fig.8 Load versus deformation curve of specimen S2

Specimen S3, with a longer 675 mm UHPC layer, represents a further refinement in the retrofitting strategy. Figure 9 and Table 4 reveal that S3 exhibits an even more pronounced increase in load-carrying capacity compared to both S1 and S2. The initial linear elastic behavior is again comparable to the control and shorter UHPC retrofit specimen, up to a drift of about 1%. The maximum load capacity reached is 231.4 kN at a 2.2% drift, reflecting an impressive increase of 24.5% over S1 and 5% over S2. This significant enhancement further underscores the effectiveness of UHPC reinforcement in improving the joint's strength. While the post-peak behavior of S3 shows some stiffness degradation, the more gradual decline, similar to S2, is indicative of enhanced ductility and energy dissipation characteristics. The extended UHPC layer in S3 potentially provides greater confinement and stress redistribution, which explains the further improvement in load-carrying capacity and ductility compared to the shorter UHPC retrofit in S2. However, the incremental gain from the extended UHPC length, as compared to S2, suggests a potential diminishing return on investment. The enhanced confinement and ductility in S3 likely stem from the UHPC's high compressive strength and steel fibers bridging microcracks at the joint core, though detailed microstructural insights remain limited without SEM analysis.

The drift capacity of S2 and S3 reached 6.5% (Table 4), compared to 5% for S1, indicating significant ductility enhancement from UHPC retrofitting. Energy dissipation ratio analysis was not performed due to the focus on load-displacement curves and limited resources. Future studies will assess this ratio to further validate seismic performance improvements.

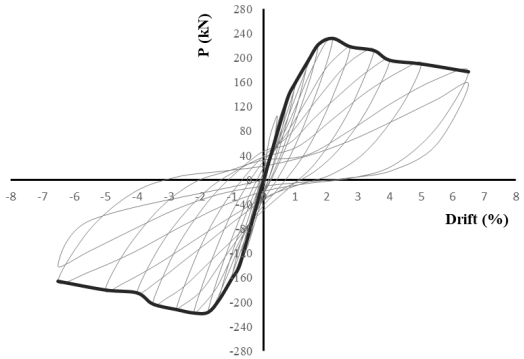

Fig.9 Load versus deformation curve of specimen S3

Overall, the comparative analysis of specimens S1, S2, and S3 reveals several key observations. The UHPC retrofit significantly enhances the load-carrying capacity of exterior beam-column joints. The increase in load capacity is directly proportional to the length of the UHPC layer, with the 675 mm retrofit (S3) yielding the highest peak load. The enhanced performance is attributed to the superior mechanical properties of UHPC, such as its high compressive strength and tensile strength. The incorporated steel fibers in the UHPC further enhance the ductility and energy dissipation capacity of the joint by bridging cracks and resisting tensile stresses. The results support the hypothesis that UHPC is an effective material for retrofitting existing reinforced concrete structures, particularly when the objective is enhanced seismic performance. These enhancements align with Eurocode 8's ductility demands and echo Sharma et al. [28] and Khan et al. [29], confirming UHPC's seismic retrofit efficacy.

It should be noted that, to analyze these outcomes, load-displacement data were evaluated using basic statistical measures like peak load averages and drift comparisons, though detailed statistical methods or other quantitative analyses were not applied. To check these results, they were compared with other studies. Sharma et al. [28] found better ductility and strength in UHPC-retrofitted joints, similar to this study's findings for S2 and S3. Khan et al. [29] also reported up to 25% higher load capacity with UHPC, close to the 24.5% increase in S3. However, the small 5% gain from S2 to S3 suggests that longer UHPC layers may not always be worth it, a point less discussed in earlier work. Despite these improvements, limitations exist: UHPC's higher material costs raise questions about its economic viability, and whether the performance gains justify

the expense remains unclear without cost-benefit analysis. Additionally, the modest 5% load increase from S2 to S3 suggests diminishing returns with longer UHPC layers, potentially limiting scalability.

5. CONCLUSIONS

The load-carrying capacity of the strengthened specimen S2 increased by 16% in compression and 17.6% in tension. Similarly, specimen S3 exhibited increases of approximately 20% in compression and 19.3% in tension compared to the control specimen S1. These results clearly demonstrate the significant influence of UHPSFRC strengthening on structural load capacity.

Specimens S2 and S3, incorporating UHPSFRC within the joint core, achieved their maximum load at a 2.2% drift, similar to specimen S1, albeit with different load magnitudes. Specimen S1 reached a maximum load of 185.8 kN with a maximum displacement of 91.25 mm (5% drift), while specimens S2 and S3 attained 220.8 kN and 231.4 kN, respectively, with maximum displacements of 118.6 mm (6.5% drift). According to ACI Committee 374 [37], a maximum allowable drift of 4% is generally required for building structures to ensure stability. Therefore, specimens S2 and S3 meet this criterion.

The use of UHPSFRC mitigated the challenges associated with congested reinforcement and difficult concrete placement within the joint region. Furthermore, this strengthening method enhanced the structure's load-bearing capacity, addressing practical construction considerations. These improvements align well with expectations, as UHPSFRC's superior strength and ductility were anticipated to enhance joint performance under cyclic loading. This study effectively addresses the research gaps noted in the introduction, particularly the limited knowledge of UHPSFRC's impact on the cyclic load-drift behavior of exterior beam-column joints. Regarding cost-effectiveness, UHPSFRC's higher initial material costs may be offset by reduced reinforcement needs and improved durability, though a detailed economic analysis is beyond this study's scope. However, disadvantages such as higher costs and challenges in field application, like achieving consistent bonding in varied conditions, could hinder its practical use. While UHPSFRC shows promise, its feasibility for large-scale adoption remains uncertain without further evaluation of economic and logistical factors. Besides that, this study is limited by its focus on only three full-scale specimens, which may not fully represent the variability in practical structure conditions. Additionally, the long-term durability of UHPSFRC under sustained seismic exposure remains unaddressed. Although UHPSFRC improved load capacity by 18.9% and 24.5% for S2 and S3, fatigue behavior was not studied due to equipment and time constraints, focusing instead on immediate seismic performance; future research should explore fatigue to assess long-term applicability. Based on the current findings, UHPC cannot yet be universally recommended for large-scale use in retrofitting exterior beam-column joints due to its high material costs, diminishing returns with increased retrofit length (e.g., only a 5% load capacity gain from S2 to S3), and unresolved logistical challenges such as field application consistency; however, it can be selectively recommended for critical structures in high-seismic zones where enhanced performance justifies the investment, pending further cost-benefit and scalability studies.

Further research and additional experimental validation are necessary before recommending the widespread adoption of UHPSFRC in beam-column joints. FEA validation, omitted here due to constraints, is planned for future studies to confirm findings. Further research on fatigue, cost-effectiveness, and scalability is needed. Furthermore, while UHPC mitigated reinforcement congestion in S2 and S3, improving construction efficiency, a life-cycle cost analysis (LCCA) comparing UHPC to traditional retrofitting methods (e.g., FRP, steel jacketing) was beyond this study's scope. Future research will incorporate LCCA to evaluate long-term cost-effectiveness and practicality for large-scale seismic retrofitting, complementing UHPC's proven seismic performance enhancements.

6. REFERENCES

[1] Hu B., Lv H.L., and Kundu T., Experimental study on seismic behavior of reinforced concrete frame in primary and middle schools with different strengthening methods, Construction and Building Materials, Vol. 217, 2019, pp. 473–486.

[2] Ghobarah A., Saatcioglu M., and Nistor I., The impact of the 26 December 2004 earthquake and tsunami on structures and infrastructure, Engineering Structures, Vol. 28, Issue 2, 2006, pp. 312–326.

[3] Gunaselvi S., Indumathy M., and Sivasankar S., Experimental assessment of RC beam-column connections with internal and external strengthening techniques, Materials Today: Proceedings, Vol. 27, 2020, pp. 1210–1217.

[4] Pampanin S., Calvi G.M., and Moratti M., Seismic Behabiour of RC Beam-Column Joints Designed for Gravity Loads, 12th European Conference on Earthquake Engineering, Vol. 28, Issue 3, 2002, pp. 1–13.

[5] Tran T. H., and Nguyen V. T., Seismic performance enhancement of RC beam-column joints using UHPC retrofitting: An experimental study, International Journal of GEOMATE, Vol. 24, Issue 103, 2023, pp. 45–53.

[6] Sasmal S., Novák B., Ramanjaneyulu K., et al., Seismic retrofitting of damaged exterior beam–column joints using fibre reinforced plastic composite–steel plate combined technique, Structure and Infrastructure Engineering, Vol. 9, Issue 2, 2013, pp. 116–129.
[7] Hung C.C., Hsiao H.J., Shao Y., and Yen C.H., A comparative study on the seismic performance of RC beam-column joints retrofitted by ECC, FRP, and concrete jacketing methods, Journal of Building Engineering, Vol. 64, 2023, pp. 105691.
[8] Yang L., Wu T., and Zhao M., Energy dissipation capacity of UHPC-strengthened exterior joints under seismic loading, Structures, Vol. 54, 2023, pp. 789–801.
[9] Huang Y., and Zhang B., Long-term performance of UHPC in seismic retrofitting: Experimental and numerical insights, Case Studies in Construction Materials, Vol. 18, 2023, pp. e01923.
[10] [Farhang K., Farahbod F., and Firoozi Nezamabadi M., Hysteresis behavior of 3D RC exterior beam-column joints strengthened with CFRP sheets and spike anchors, Structures, Vol. 40, 2022, pp. 1065–1077.
[11] Ghobarah A. and Said A., Shear strengthening of beam-column joints, Engineering Structures, Vol. 24, Issue 7, 2002, pp. 881–888.
[12] Le Q. H., and Pham T. D., Influence of fiber content on the cyclic behavior of UHPC-strengthened exterior joints, International Journal of GEOMATE, Vol. 25, Issue 107, 2023, pp. 67–74.
[13] Akhlaghi A. and Mostofinejad D., Experimental and analytical assessment of different anchorage systems used for CFRP flexurally retrofitted exterior RC beam-column connections, Structures, Vol. 28, 2020, pp. 881–893.
[14] Maheri M.R. and Torabi A., Retrofitting external RC beam-column joints of an ordinary MRF through plastic hinge relocation using FRP laminates, Structures, Vol. 22, 2019, pp. 65–75.
[15] Engindeniz M., Kahn L.F., and Zureick A.H., Pre-1970 Rc Corner Beam-Column-Slab Joints: Seismic Adequacy and Upgradeability With Cfrp Composites, 14th World Conference on Earthquake Engineering (14WCEE), 2008, pp. 1–8.
[16] Al-Salloum Y., Almusallam T., Alsayed S., and Siddiqui N., Seismic behavior of as-built, ACI-complying, and CFRP-repaired exterior RC beam-column joints, Journal of Composites for Construction, Vol. 15, 2011, pp. 522–534.
[17] Röhm C., Novák B., Sasmal S., et al., Behaviour of fibre reinforced beam-column sub-assemblages under reversed cyclic loading, Construction and Building Materials, Vol. 36, 2012, pp. 319–329.
[18] IS-1893-Part-1, Criteria for Earthquake Resistant Design of Structures - General Provisions and Buildings Part-1, Bureau of Indian Standards, New Delhi, Part 1, 2002, pp. 1–39.
[19] Dao N. T., and Bui V. H., Finite element modeling of UHPC-strengthened exterior joints under reversed cyclic loading, International Journal of GEOMATE, Vol. 25, Issue 106, 2023, pp. 12–19.
[20] Vu T. A., and Hoang L. P., Durability assessment of UHPC-retrofitted beam-column joints under seismic loading, International Journal of GEOMATE, Vol. 26, Issue 109, 2024, pp. 23–30.
[21] Antonopoulos C.P. and Triantafillou T.C., Experimental Investigation of FRP-Strengthened RC Beam-Column Joints, Journal of Composites for Construction, Vol. 7, Issue 1, 2003, pp. 39–49.
[22] Lim, J. H. and Tan C. S., Mechanical properties and failure modes of UHPC under high strain rates, Materials Today: Proceedings, Vol. 65, 2022, pp. 2345–2352.
[23] Alsomiri M., Liu Z., Abadel A.A., and Li M., Revision and development of material models of ultra-high performance concrete containing coarse aggregate and applications in structural-level flexural response predictions, Structures, Vol. 51, 2023, pp. 332–350.
[24] Yu L., Bai S., and Guan X., Effect of multi-scale reinforcement on fracture property of ultra-high performance concrete, Construction and Building Materials, Vol. 397, 2023, pp. 132383.
[25] Hussein H.H., Sargand S.M., Zhu Y., et al., Experimental and numerical investigation on optimized ultra-high performance concrete shear key with shear reinforcement bars, Structures, Vol. 40, 2022, pp. 403–419.
[26] Qian Y., Yang D., Xia Y., Gao H., and Ma Z., Properties and improvement of ultra-high performance concrete with coarse aggregates and polypropylene fibers after high-temperature damage, Construction and Building Materials, Vol. 364, 2023, pp. 129925.
[27] Limpaninlachat P., Kunawisarut A., Van Hong Bui L., et al., Flexural and shear behavior of ultra-high performance concrete segmental joints, Structures, Vol. 56, 2023, pp. 104913.
[28] Sharma R. and Bansal P.P., Behavior of RC exterior beam column joint retrofitted using UHP-HFRC, Construction and Building Materials, Vol. 195, 2019, pp. 376–389.
[29] Khan M.I., Al-Osta M.A., Ahmad S., and Rahman M.K., Seismic behavior of beam-column joints strengthened with ultra-high performance fiber reinforced concrete, Composite Structures, Vol. 200, 2018, pp. 103–119.
[30] Huang L., Du Y., Zhu S., and Wang L., Material property and constitutive model of C120 hybrid fiber ultra-high performance concrete at elevated temperatures, Structures, Vol. 50, 2023, pp. 373–386.
[31] Gurusideswar S., Shukla A., Jonnalagadda K.N., and Nanthagopalan P., Tensile strength and failure of ultra-high performance concrete (UHPC) composition over a wide range of strain rates, Construction and Building Materials, Vol. 258, 2020, pp. 119642.
[32] Ding Y., Zeng B., Zhou Z., Wei Y., and Huang Y., Behavior of UHPC columns confined by high-strength transverse reinforcement under eccentric compression, Journal of Building Engineering, Vol. 70, 2023, pp. 106352.

[33] Fu T., Wang K., Zhu Z., et al., Seismic performance of prefabricated square hollow section piers strengthened by jacketing using UHPC and high-strength steel, Structures, Vol. 47, 2023, pp. 449–465.
[34] Puskas A. and Moga L.M., Sustainability of reinforced concrete frame structures - A case study, International Journal of Sustainable Development and Planning, Vol. 10, Issue 2, 2015, pp. 165–176.
[35] Zhao B., Taucer F., and Rossetto T., Field investigation on the performance of building structures during the 12 May 2008 Wenchuan earthquake in China, Engineering Structures, Vol. 31, Issue 8, 2009, pp. 1707–1723.
[36] Beschi C., Riva P., Metelli G., and Meda A., HPFRC Jacketing of non seismically detailed RC corner joints, Journal of Earthquake Engineering, Vol. 19, 2014, pp. 25–47.
[37] Hakuto S., Park R., and Tanaka H., Seismic load tests on interior and exterior beam-column joints with substandard reinforcing details, ACI Structural Journal, Vol. 97, 2000, pp. 11–25.
[38] Nguyen H. M. and Tran, D. K., Cost-effectiveness analysis of UHPC in seismic retrofitting of RC structures, International Journal of GEOMATE, Vol. 24, Issue 105, 2023, pp. 89–96.
[39] Eurocode 8, Design provisions for earthquake resistance of structures, British Standards Institution London, 1998, London SE.